Available online at www.sciencedirect.com
SCIENCE DIRECT®
Journal of Catalysis 230 (2005) 1–13
JOURNAL OF CATALYSIS
www.elsevier.com/locate/jcat

Selective catalytic oxidation of ammonia to nitrogen at low temperature on $Pt/CuO/Al_2O_3$

Göran Olofsson [a], L. Reine Wallenberg [b], Arne Andersson [a,*]

[a] *Department of Chemical Engineering, Chemical Center, Lund University, Box 124, SE-221 00 Lund, Sweden*
[b] *Department of Materials Chemistry/nCHREM, Chemical Center, Lund University, Box 124, SE-221 00 Lund, Sweden*

Received 7 September 2004; revised 12 November 2004; accepted 16 November 2004

Abstract

$Pt/CuO/Al_2O_3$ catalysts with 20 wt% CuO and 0.5–4 wt% Pt were prepared and used for the selective catalytic oxidation of ammonia in wet and dry gases and in synthetic biogas with CO, hydrogen, and methane. Imaging of the catalysts with HREM and STEM, combined with elemental analysis, reveals that copper is well dispersed and occurs in the form of patches on the support. Platinum in the form of nanometer-sized particles are localised on copper-rich areas. The activity measurements show that $Pt/CuO/Al_2O_3$ is active and selective for the oxidation of ammonia to form nitrogen. Compared with dry feeds, the catalyst shows higher selectivity for nitrogen when the feed is wet. Pretreatment of the catalyst with SO_2-containing gas produces an improved catalyst with a selectivity for nitrogen of about 97–98% at complete ammonia conversion. $Pt/CuO/Al_2O_3$ shows good performance also for the oxidation of ammonia to nitrogen in the presence of biogas components including water. However, the performance is not as good under dry conditions, giving either low selectivity for nitrogen or low conversion of the ammonia, depending on the partial pressure of oxygen.

Keywords: Selective catalytic oxidation; SCO; Ammonia; $Pt/CuO/Al_2O_3$ catalysts; Dry feed; Wet feed; Sulphating; Biogas components; HREM; STEM

1. Introduction

The abatement of ammonia from industrial waste gas streams is becoming increasingly important because of environmental concerns. Depending on the application, various techniques can be used for the removal of ammonia, such as adsorption, absorption, chemical treatment, catalytic decomposition, and selective catalytic oxidation (SCO) to form nitrogen and water. The last technique is attractive, especially for treatment of large gas flows containing oxygen and a low concentration of ammonia. The application area for SCO includes the treatment of waste gases from chemical production processes, SCR facilities, and gasification/combustion of biomass for combined heat and power generation. Another application area that might be important in the future concerns the use of biogas for synthesis purposes. In the gasification of biomass, the fuel-bound nitrogen is released predominantly as ammonia, which in combined heat and power production should be removed prior to the gas turbine [1]. Thus, a catalyst operating at high temperatures (∼ 700 °C) would give the best process efficiency. On the other hand, in other applications it is usually desirable to have a catalyst operating at lower temperatures, for example, in SCR facilities where ammonia is fed to react with NO_x on a catalyst to give nitrogen. Here the degree of NO_x conversion is limited because any trace of ammonia has to be avoided. Therefore, a NH_3/NO_x molar ratio of about 0.9 is usually not exceeded. The NO_x removal efficiency would be improved if one could use a secondary SCO catalyst bed to efficiently convert an added small excess of ammonia to nitrogen under SCR conditions. However, the difficulty is that the SCO catalyst has to be effective below 300 °C, as in many other applications in the presence of high concen-

---

[*] Corresponding author.
E-mail address: Arne.Andersson@chemeng.lth.se (A. Andersson).

0021-9517/$ – see front matter
doi:10.1016/j.jcat.2004.11.023

trations of water [2]. Furthermore, it is necessary to achieve almost 100% conversion of the ammonia to avoid odour [3].

Platinum is active for ammonia oxidation and is used as a catalyst in the first step in nitric acid production to oxidise ammonia to NO at 800–900 °C [4]. At temperatures below 300 °C platinum produces nitrogen rather than NO [5], but the selectivity is comparatively low since high levels of N_2O are co-produced [2]. Examples of more promising catalyst systems for the SCO of ammonia are (i) the supported oxide systems MoO_3/SiO_2 [6,7], V_2O_5/TiO_2 [2,8], CuO/TiO_2 [8], CuO/Al_2O_3 [9,10], NiO/Al_2O_3 [11], and Fe_2O_3/TiO_2 [12]; (ii) the ion-exchanged zeolite systems Cu-ZSM-5 [8,13], Cu-Y-zeolite [9], Pd-ZSM-5 [2], and Fe-ZSM-5 [13,14]; and the supported oxide systems with a precious metal component, $Pd–V_2O_5–WO_3/TiO_2–SiO_2$ [3], $Ir–V_2O_5–WO_3/TiO_2–SiO_2$ [3], $Ag/CuO/Al_2O_3$ [15,16], and $Au/CuO/Al_2O_3$ [17]. Considering the desired target of both complete conversion of ammonia and high selectivity for nitrogen, a problem with most of these catalyst systems is that they have to be used at temperatures well above 300 °C, and the selectivity for nitrogen formation decreases with increasing temperature and conversion. For use in SCR applications the target temperature is below 300 °C, and thus there is a need for more efficient low-temperature catalysts. The addition of a precious metal component to supported oxides seems beneficial [3,15–17]; for example, $Ag/CuO/Al_2O_3$ has been reported to give complete conversion of ammonia at 250 °C with a high selectivity for nitrogen [15]. A problem here is that the space velocity has to be low, around 450 ml/(min g) of catalyst, compared with 1000–5000 ml/(min g) for the other catalyst systems. Therefore, it is of interest that $Pt/CuO/Al_2O_3$ has been reported to be active and selective for nitrogen formation at 200 °C at a space velocity of about 5000 ml/(min g) when it is used for ammonia oxidation in dry biogas with low oxygen content [18]. For combined heat and power generation a temperature of 200 °C is not optimal since higher temperatures are preferred [1], but doubtlessly the $Pt/CuO/Al_2O_3$ system has a potential for low-temperature applications.

In the present study, to further explore the $Pt/CuO/Al_2O_3$ catalyst system, samples with various platinum contents have been prepared and used for the selective catalytic oxidation of ammonia to nitrogen under both dry and wet conditions and with different oxygen contents in the gas. Moreover, as waste gases may contain SO_2, the influence of SO_2 treatment on the performance of the catalyst has been investigated. It has been reported for ammonia oxidation on CuO/TiO_2 [8], CuO/Al_2O_3 [10], Fe-ZSM-5 [13], and Fe_2O_3/TiO_2 [12] that sulphate species may improve the selectivity for nitrogen. In a patent [19] data are presented showing that sulphating of, for example, a $Pt/CuO/SiO_2$ catalyst has a remarkable effect on the selectivity for nitrogen. Another aim of the present investigation was to collect data for ammonia oxidation in the presence of biogas components (CO, H_2, CH_4) by FTIR analysis of the product stream. In the previous investigation [18] of the same catalyst system, mass spectrometric analysis was performed without separation of the components with overlapping mass signals (CO_2/N_2O and CO/N_2).

2. Experimental

2.1. Catalyst preparation

Four different $Pt/CuO/Al_2O_3$ catalysts were prepared with 20 wt% CuO and with 0.5, 1, 2, and 4 wt% Pt, respectively. CuO/Al_2O_3 was synthesised first, and, in a second step, the desired amount of Pt was deposited. CuO/Al_2O_3 was prepared by incipient wetness impregnation of Al_2O_3 (Condea, 119 m^2/g) with a water solution of $Cu(NO_3)_2 \cdot 3H_2O$ (Merck, p.a.). The sample was dried for 5 h under ambient conditions, followed by another 24 h at 120 °C. Subsequently, the sample was calcined in air with ramping temperature. Primarily, the temperature was increased by 10 °C/min up to 300 °C, where the sample was held for 1 h. In this step most of the nitrate decomposed to form nitrogen oxides. The temperature was thereafter increased by 10 °C/min up to 500 °C, where it was kept constant for 6 h. For preparation of $Pt/CuO/Al_2O_3$, 3 g of the as-prepared CuO/Al_2O_3 sample was immersed in the desired amount of Pt(II) nitrate solution (Heraeus, 15.46 wt% Pt) diluted with water to give a total volume of 40 ml. The slurry was stirred repeatedly for 1 h to ensure that practically all of the Pt was adsorbed on CuO/Al_2O_3. The $Pt/CuO/Al_2O_3$ precursors were dried and calcined with the same procedure as that used for CuO/Al_2O_3, with the exception that the final calcination temperature was 450 °C instead of 500 °C. After calcination, the samples were crushed and sieved. The fraction of particles with diameters in the 250–425-µm range was collected and used in the experiments.

2.2. Activity measurements

The activity measurements were carried out in a stainless-steel plug-flow reactor with an inner diameter of 1.9 mm. The reactor was placed in a GC-type electric furnace equipped with a temperature control. An Environics series 2000 computerised multicomponent gas mixer was used to prepare the inlet gas mixtures, consisting of NH_3 and O_2 in N_2 with or without water vapour and biogas components (CO, H_2, and CH_4). For analysis of the inlet and product gases a GASMET FT-IR gas analyser was used, which permitted an analysis of NH_3, N_2O, NO, NO_2, CO, CO_2, CH_4, and H_2O. The formation of N_2 and the consumption of H_2 were obtained from the mass balance for N and H, respectively, over the reactor. All feed gases (1.48 ± 0.04 vol% NH_3 in He, O_2, N_2, CO, H_2, and CH_4) were high purity grade supplied by AGA. The conversion of NH_3 and the selectivity for N_2, N_2O, NO, and NO_2 were measured on the catalysts for different gas compositions and temperatures. In the experiments the total inlet gas flow was 1000 Nml/min, the temperature was varied between 150 and 335 °C, and the amount of catalyst was 0.20–0.35 g. Before the measurements the catalyst was pretreated at 235 °C for 16 h under a gas flow of 1000 Nml/min containing 700 ppm NH_3 and 8.0 vol% O_2 in N_2. After this treatment, in some experiments, the catalyst was subjected for another 30 min to the former gas with an additional 100 ppm SO_2.

2.3. Catalyst characterisation

The specific surface areas of the samples were obtained from a multipoint Brunauer–Emmet–Teller (BET) analysis of the nitrogen adsorption isotherm, recorded on a Micromeritics ASAP 2400 instrument at liquid nitrogen temperature. All samples were degassed under vacuum at 350 °C for 16 h before analysis. Specific surface areas and notation of the samples are given in Table 1.

Temperature-programmed desorption (TPD) experiments were performed with a TAP-2 reactor system with a microreactor connected to a UTI 100C mass spectrometer [20]. Fifty milligrams of catalyst was loaded between inert layers of quartz sand of the same particle size. Before the experiment was started, the catalyst was heated for 10 min at 350 °C with pure O_2 flowing through the reactor (40 Nml/min), cooled down to 50 °C, and evacuated. Then, a flow with 20 vol% NH_3 in Ar (58 Nml/min) was passed through the sample for 30 min. After evacuation of the reactor, the temperature was increased linearly by 10 °C/min from 50 up to 350 °C. Simultaneously, the mass signals from NH_3 (17 amu), H_2O (17 and 18 amu), H_2 (2 amu), N_2 (28 amu), N_2O (28, 30 and 44 amu), NO (30 amu), and NO_2 (30 and 46 amu) were registered and used for calculation of the desorption profiles.

Table 1
Notation, composition and specific surface area of prepared $Pt/CuO/Al_2O_3$ catalysts and the Al_2O_3 support

Sample	Pt (wt%)	CuO (wt%)	Specific surface area (m^2/g)
Al_2O_3	–	–	119
0.5 wt% $Pt/CuO/Al_2O_3$	0.5	20	99
1 wt% $Pt/CuO/Al_2O_3$	1	20	94
2 wt% $Pt/CuO/Al_2O_3$	2	20	100
4 wt% $Pt/CuO/Al_2O_3$	4	20	99

X-ray diffraction (XRD) analysis was carried out on a Seifert XRD 3000 TT diffractometer with monochromatic Cu-K_α radiation (50 kV/30 mA). The scanning range was 2.5–40° (Θ) with a step size of 0.01° and a step time of 1.0 s. Compound identification was accomplished by comparison with the JCPDS data file [21]. The measurements were performed on ground samples with the use of a rotating sample holder.

Temperature-programmed reduction (TPR) was performed on a Micromeritics TPD/TPR 2900 instrument. The temperature was increased by 10 °C/min from 40 to 900 °C. The reducing gas was 8.5 vol% H_2 in Ar, and a flow rate of 40 ml/min was used. The water produced during the reduction process was condensed in a cold trap at about −90 °C. The 4-mm quartz tube reactor was loaded with ~ 20 mg of sample with particle sizes in the range of 250–425 µm.

High-resolution transmission electron microscopy (HREM) and elemental analysis were performed with a JEM 3000F field-emission microscope equipped with an Oxford energy-dispersive X-ray spectrometer (XEDS). The microscope was operated at 300 kV in both conventional and scanning mode. A Fischione high-angle annular dark-field detector (HAADF) was used for selective imaging of platinum particles on the support. Mo grids with a continuous amorphous carbon film were used, rather than the usual Cu grids, to eliminate spurious Cu radiation from the background. The resolution of the microscope is 0.162 nm in conventional HREM imaging and 0.14 nm in STEM mode. A probe size of 0.2–0.7 nm was used for imaging, and 1.0 nm for XEDS mapping.

3. Results

3.1. TPD of adsorbed ammonia

Fig. 1 displays the TPD profiles of ammonia and formed products as obtained after ammonia is adsorbed at 50 °C on

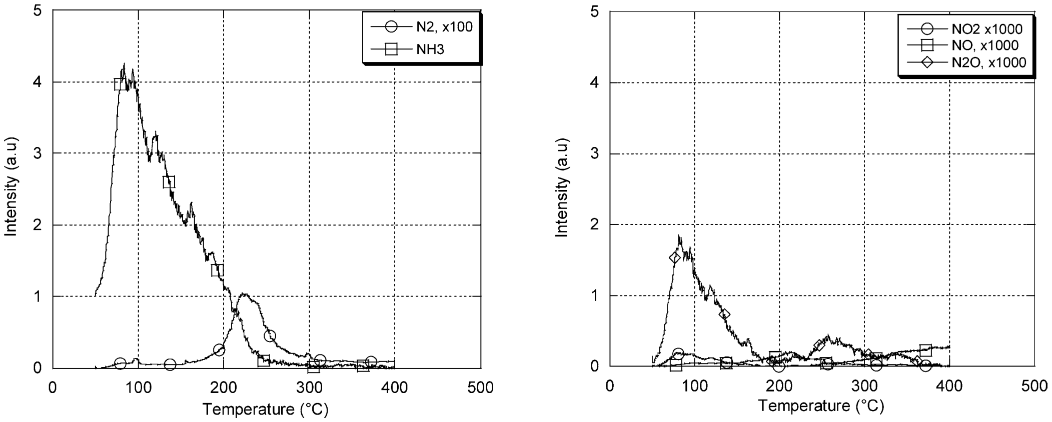

Fig. 1. TPD profiles of ammonia and formed products as recorded after adsorption of ammonia at 50 °C on the preoxidised 1 wt% $Pt/CuO/Al_2O_3$.

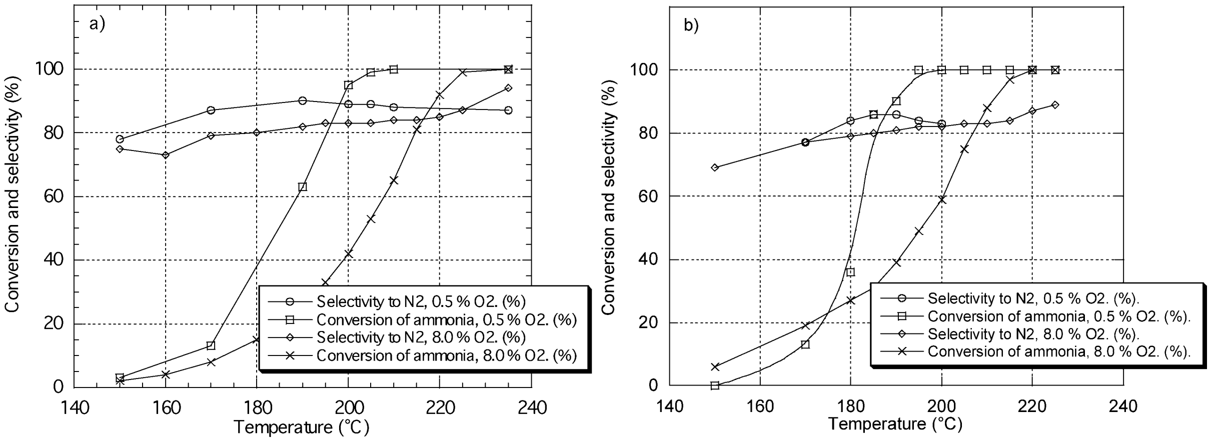

Fig. 2. A comparison of (a) 1 wt% $Pt/CuO/Al_2O_3$ and (b) 4 wt% $Pt/CuO/Al_2O_3$ for the selective catalytic oxidation of ammonia to produce nitrogen. Feed: 700 ppm NH_3 and either 0.5 or 8.0 vol% O_2 in N_2. Space velocity: 3000 ml/(min g_{cat}).

1 wt% $Pt/CuO/Al_2O_3$. The figure shows that desorption of ammonia occurs from low temperatures up to 250 °C, with a maximum at about 80 °C. This feature shows that ammonia is comparatively strongly adsorbed at 50 °C. In parallel with the ammonia desorption, formation and desorption of hydrogen were observed, indicating that upon heating some of the adsorbed ammonia was activated and transformed into an NH_x type of species. Some of the hydrogen formed reacts with oxygen to produce water, as was noted by the resemblance of the hydrogen and water profiles.

The nitrogen profile in Fig. 1 presents a maximum at 225 °C. Of the nitrogen oxides, N_2O gives a major peak extending from low temperatures up to 200 °C. Compared with the nitrogen peak, this peak is small. Almost no formation of NO_2 and NO is observed in the experiment. The TPD profiles demonstrate that $Pt/CuO/Al_2O_3$ is active and selective for nitrogen formation in a window around 225 °C, which thus would be the most suitable temperature for use of the catalyst.

3.2. Catalyst ignition profiles

The oxidation of ammonia was studied over 1 and 4 wt% $Pt/CuO/Al_2O_3$ at temperatures from 150 °C up to around 230 °C. A feed with 700 ppm ammonia and either 0.5 or 8.0 vol% oxygen in nitrogen was passed over the catalyst at 3000 ml/(min g) in space velocity. The results are plotted in Fig. 2. The graphs show that the conversion of ammonia increases with the temperature. Compared with the conversions that are obtained with 8.0 vol% oxygen in the feed, both catalysts generally give higher conversions for the feed with 0.5 vol% oxygen. Moreover, an increase in the Pt content in the catalyst from 1 to 4 wt% has a modest influence on the activity. For the feed with 8.0 vol% oxygen, complete conversion of ammonia over 1 wt% $Pt/CuO/Al_2O_3$ and 4 wt% $Pt/CuO/Al_2O_3$ is obtained at 230 and 220 °C, respectively, compared with 210 and 195 °C, respectively, for the feed with 0.5 vol% oxygen. The selectivity for nitrogen formation shows the same type of behaviour with temperature for both catalysts. At the highest oxygen content the selectivity increases with the temperature, whereas at the lowest oxygen content, the selectivity passes through a weak maximum. At low temperatures the selectivity generally is the highest for the lowest oxygen content. The selectivity for nitrogen on both catalysts is about 85–90% at complete ammonia conversion.

3.3. Influence of the temperature and the oxygen content on the selectivity for nitrogen at high ammonia conversion

The catalytic performance was investigated for a feed with 700 ppm ammonia at varying temperatures from 210 to 335 °C and different oxygen concentrations (0.5–20.0 vol%) in the feed. Fig. 3 displays the selectivity dependences for nitrogen formation on 1 wt% $Pt/CuO/Al_2O_3$. The catalyst is highly active and the conversion is above 99% at all temperatures except 210 °C. For the two lowest oxygen concentrations, 0.5 and 1.0 vol% (Figs. 3a and 3b), the selectivity for nitrogen decreases with increasing temperature, whereas for higher oxygen concentrations (2.0–20.0 vol%) it passes through a maximum (Figs. 3c–3f). However, as can be seen in Fig. 2, at lower temperatures there is a selectivity maximum also for the lowest oxygen concentration. The temperature for the maximum seems to shift towards higher temperatures with increasing oxygen content in the gas. A comparison of the data for 210 and 335 °C in Figs. 3a–3f reveals that the selectivity for nitrogen decreases with increasing oxygen concentration. At 210 °C the selectivity drops from 88 to 77% when the oxygen concentration is increased from 0.5 to 20.0 vol%. The corresponding decrease at 335 °C is from 85 to 68%. In the whole range of oxygen concentrations, however, at intermediate temperatures ($\sim$ 260 °C) the selectivity for nitrogen is about 85% at complete ammonia conversion.

The by-products formed over $Pt/CuO/Al_2O_3$ are NO, NO_2 (NO_x), and N_2O. The formation of the respective product depends on the temperature and the oxygen concentration in the gas, as illustrated in Fig. 4. With low oxygen

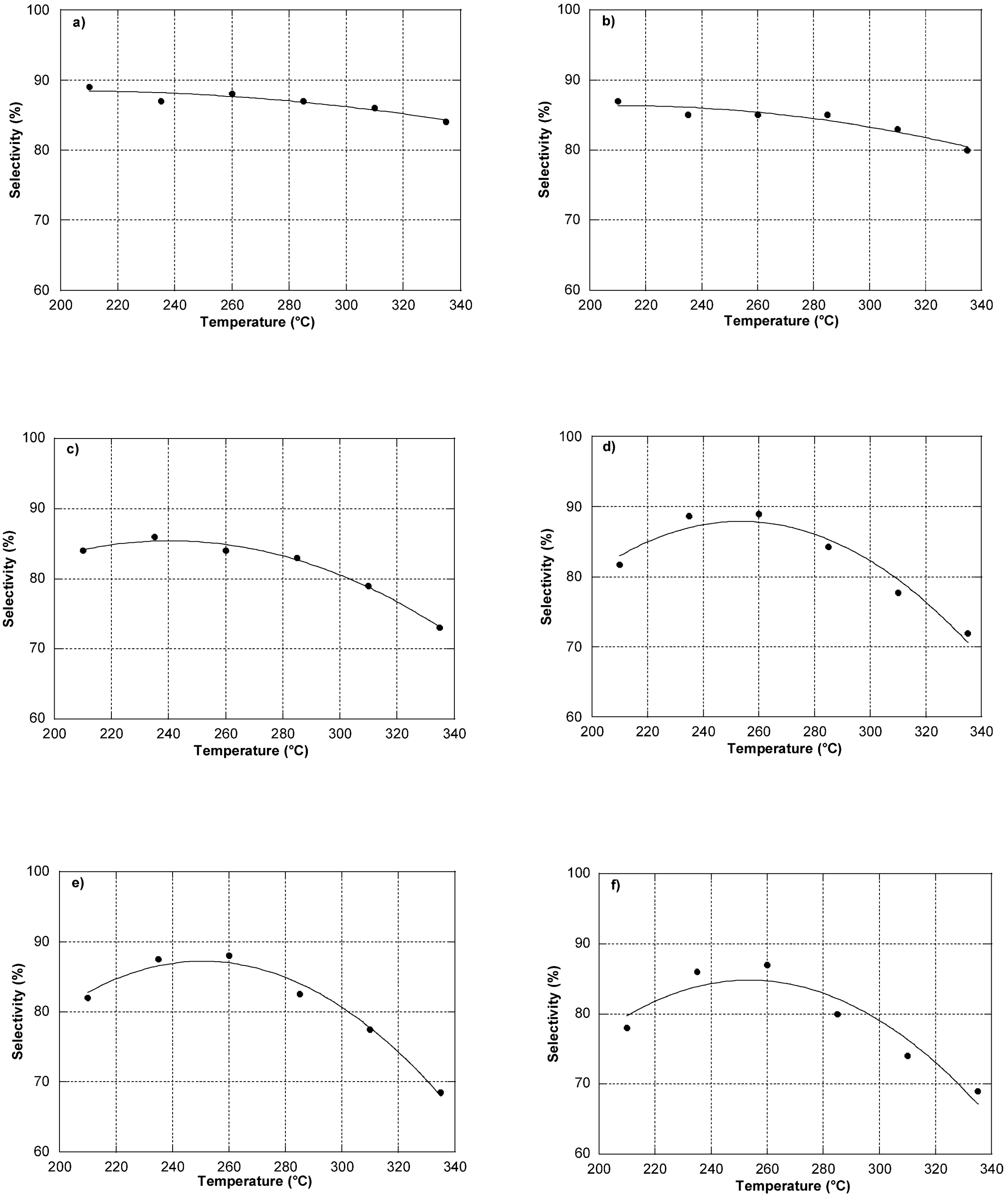

Fig. 3. The influence of the temperature and the oxygen concentration on the selectivity to nitrogen formation in ammonia oxidation on 1 wt% $Pt/CuO/Al_2O_3$. Space velocity: 3000 ml/(min g_{cat}). Feed: 700 ppm NH_3 and (a) 0.5, (b) 1.0, (c) 2.0, (d) 4.0, (e) 8.0, and (f) 20.0 vol% O_2 in N_2.

content in the gas (Fig. 4a), N_2O and NO are the major by-products. In the interval 210–335 °C the selectivity for N_2O is almost constant at $\sim 9\%$. Increase in the temperature leads to more NO_x being formed, with more NO than NO_2.

For feeds with high oxygen contents, the maximum in the selectivity for nitrogen (Fig. 3) is concurrent with a minimum in the amount of N_2O being produced (Fig. 4b). Compared with the data in Fig. 4a, higher selectivities for N_2O are observed for the oxygen-rich feed (Fig. 4b). Moreover, with increasing temperature the selectivity for NO_x $(NO + NO_2)$ increases up to 14% at 335 °C, compared with 8% at the lower oxygen pressure. However, in contrast to the data at low oxygen content, more NO_2 than NO is formed.

3.4. *Influence of water and CO on the performance of the catalysts for ammonia oxidation to nitrogen*

In Fig. 5 the performances of $Pt/CuO/Al_2O_3$ samples with 0.5–4.0 wt% Pt are compared for ammonia oxidation to nitrogen under dry and wet conditions, respectively. Under dry

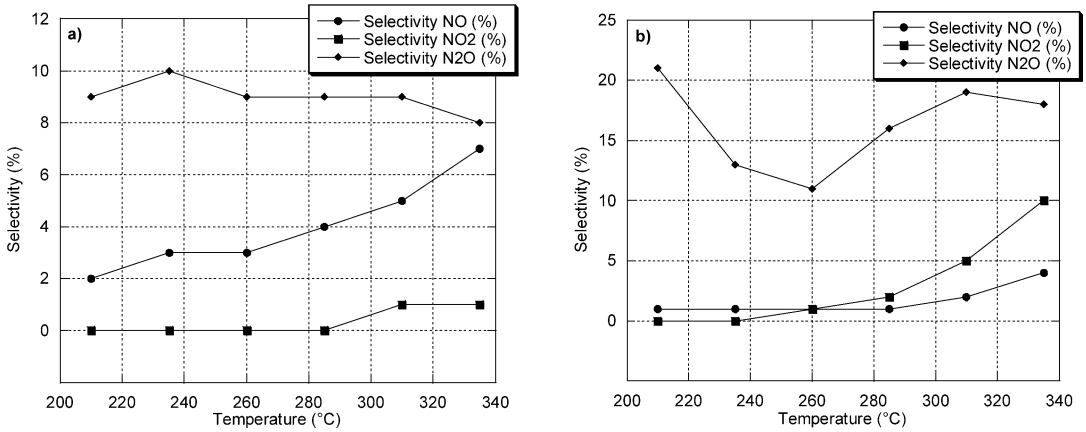

Fig. 4. Formation of N_2O, NO and NO_2 on 1 wt% $Pt/CuO/Al_2O_3$ as a function of the reaction temperature. Space velocity: 3000 ml/(min g_{cat}). Feed: 700 ppm NH_3 with (a) 0.5 and (b) 20.0 vol% O_2, respectively, in N_2.

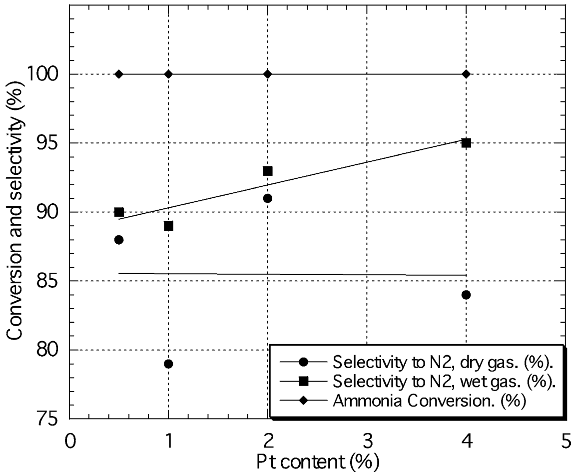

Fig. 5. A comparison of the performances of $Pt/CuO/Al_2O_3$ catalysts with different Pt contents for ammonia oxidation to nitrogen in dry and wet gas, respectively. Reaction temperature: 235 °C. Space velocity: 3600 ml/(min g_{cat}). Dry feed: 700 ppm NH_3 and 8.0 vol% O_2 in N_2. Wet feed: 700 ppm NH_3, 8.0 vol% O_2, and 8 vol% H_2O in N_2.

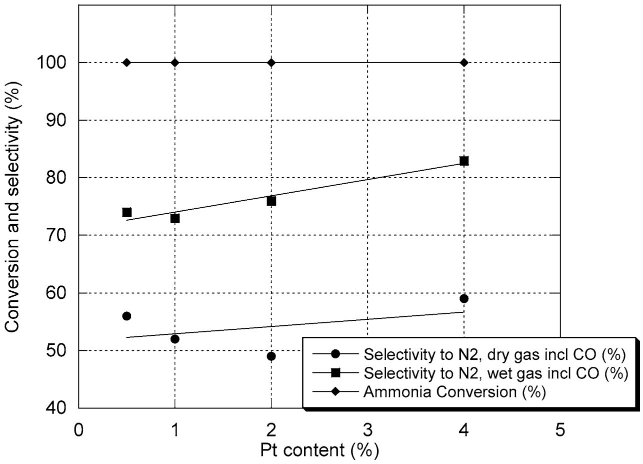

Fig. 6. A comparison of the performances of $Pt/CuO/Al_2O_3$ catalysts with different Pt contents for ammonia oxidation to nitrogen in dry and wet gas with CO. Reaction temperature: 235 °C. Space velocity: 3600 ml/(min g_{cat}). Dry feed: 700 ppm NH_3, 1.0 vol% CO and 8.0 vol% O_2 in N_2. Wet feed: 700 ppm NH_3, 1.0 vol% CO, 8.0 vol% O_2 and 8 vol% H_2O in N_2.

conditions the conversion of ammonia is almost 100% on all catalysts. Moreover, the selectivity for nitrogen is about 85% and is independent of the Pt content. It is worth pointing out that under the conditions of the experiments, the addition of water vapour to the feed has no noticeable effect on the ammonia conversion. The effect of water on the selectivity for nitrogen is minor at low Pt contents, but there is a tendency with increasing Pt content for the selectivity to increase. For 4 wt% $Pt/CuO/Al_2O_3$ the selectivity for nitrogen is 85 and 95% under dry and wet conditions, respectively.

Since industrial waste gases may contain other compounds in addition to ammonia, ammonia oxidation in the presence of CO was investigated in dry and wet gases. Fig. 6 shows data for the selectivity for nitrogen for a feed with 8.0 vol% oxygen and at the almost complete conversion of both ammonia and CO. In dry gas the selectivity for nitrogen is approximately 56%, irrespective of the Pt content of the catalyst, which is substantially lower than the 85% observed in dry gas without CO (Fig. 5). The effect of water vapour on the selectivity for nitrogen, however, is much enhanced when ammonia is fed together with CO. In wet gas the conversions of ammonia and CO apparently are unchanged, whereas the selectivity for nitrogen is increased up to the 70–80% range, depending on the Pt content. Under both wet and dry conditions, N_2O is the major by-product.

3.5. *Influence of SO_2 treatment of the catalyst*

The effect of pretreatment of the catalysts with SO_2 was investigated. Table 2 shows the performances of 1 and 4 wt% $Pt/CuO/Al_2O_3$ at high ammonia conversion in wet and dry feeds. Clearly, the data show that the pretreatment leads to a considerable improvement of the selectivity in parallel with a small decrease in the activity. For dry conditions the SO_2 treatment has no effect on the conversion, which remains practically 100%, whereas the selectivity for nitrogen

Table 2
Ammonia conversion and selectivity to nitrogen at 235 °C over Pt/CuO/Al_2O_3 catalysts in dry and wet gas before and after SO_2-treatment[a], respectively

Type of feed[b] and treatment with SO_2	1 wt% Pt/CuO/Al_2O_3		4 wt% Pt/CuO/Al_2O_3	
	Conversion (%)	Selectivity (%)	Conversion (%)	Selectivity (%)
Dry feed, untreated	100	79	100	84
Dry feed, treated	100	98	100	98
Wet feed, untreated	100	89	100	95
Wet feed, treated	97	98	100	97

[a] Pretreatment with 100 ppm SO_2 in the gas as described in Section 2.
[b] Dry feed: 700 ppm NH_3 and 8.0 vol% O_2 in N_2. Wet feed: 700 ppm NH_3, 8.0 vol% O_2 and 8 vol% H_2O in N_2. Space velocity: 3600 ml/(min g_{cat}).

Table 3
Ammonia oxidation in synthetic biogas. Conversion (Conv.) of NH_3, CO, H_2, CH_4 and selectivity (Sel.) to N_2 over 1 wt% Pt/CuO/Al_2O_3 at 235 °C and a space velocity of 3600 ml/(min g_{cat})

Feed with 700 ppm NH_3 and (%)					NH_3 (%)		Conversion (%)		
O_2	CO	H_2	CH_4	H_2O	Conv.	Sel.	CO	H_2	CH_4
0.5					100	87			
8.0					100	91			
0.5				6.5	97	94			
8.0				6.5	100	95			
0.5	1.0				52	100	54		
8.0	1.0				100	60	100		
0.5		1.0			17	100		73	
8.0		1.0			100	83		100	
0.5			1.0		100	85			0
8.0			1.0		100	91			0
0.5	1.0	1.0	1.0		18	87	38	61	0
8.0	1.0	1.0	1.0		100	55	100	96	0
0.5	1.0	1.0	1.0	7.0	100	98	54	–[a]	3
8.0	1.0	1.0	1.0	7.0	100	90	100	–[a]	3

[a] Could not be determined from the material balance for H because of the high water content in the feed.

increases from 79–84% before to 98% after the treatment. Under wet conditions a small decrease in the conversion can be noticed for 1 wt% Pt/CuO/Al_2O_3. For both catalysts the selectivity increases by a few percent and reaches about 98% after the SO_2 treatment.

3.6. *Selective catalytic oxidation of ammonia in biogas*

The oxidation of ammonia was investigated on 1 wt% Pt/CuO/Al_2O_3 in the presence of CO, hydrogen, methane, and the respective absence and presence of water. For comparisons the oxidation of ammonia was also investigated in the presence of each of the biogas components. The results are shown in Table 3. For a dry feed without fuel components, complete ammonia conversion is achieved with a selectivity for nitrogen on the order of 90%. Addition of water to the feed improves the selectivity for nitrogen. In the oxygen-rich feed (8.0 vol%) the ammonia conversion is complete (see also Fig. 5), whereas at the lower oxygen content (0.5 vol%) the addition of water causes a small decrease in the conversion. Oxidation of 700 ppm ammonia in the presence of 0.5 vol% oxygen and 1.0 vol% CO gives ammonia and CO conversions on the order of 50%. The selectivity for nitrogen is 100%. When the oxygen concentration in the feed is increased to 8.0 vol% the conversion of both ammonia and CO is complete. In this case, however, the formation of N_2O is increased and the selectivity for nitrogen drops to 60% (see also Fig. 6). Oxidation of the ammonia in a gas with 0.5 vol% oxygen and 1.0 vol% hydrogen gives 17% ammonia conversion, compared with 73% conversion of the hydrogen. Increase of the oxygen content in the feed to 8.0 vol% results in complete conversion of both hydrogen and ammonia, with a selectivity for nitrogen of 83%, compared with 100% for the lower oxygen content. For the feeds with ammonia and methane, no conversion of the methane is observed, and the oxidation of ammonia is complete at both oxygen levels. The selectivity for nitrogen seems to be unaffected by the presence of methane, and the values are almost identical to those obtained for the feeds with ammonia and oxygen only.

For dry biogas with ammonia, CO, hydrogen, methane, and 0.5 vol% oxygen, no conversion of methane is obtained, and the conversions of ammonia, CO, and hydrogen are 18, 38, and 61%, respectively, corresponding to almost complete consumption of the oxygen in the feed. The selectivity for nitrogen formation is 87%. Increase in the oxygen content to 8.0 vol% leads to the almost complete conversion of ammonia, CO, and hydrogen, whereas methane passes unconverted. The selectivity for nitrogen drops to 55%. Compared with dry conditions, both the ammonia conversion and the selectivity for nitrogen are enhanced when there is water in the feed. At both 0.5 and 8.0 vol% oxygen, full conversion of the ammonia is obtained. The selectivity for nitrogen decreases from 98 to 90% with increasing oxygen concentration in the feed. Comparison of the respective data in Table 3 for wet and dry biogas with 0.5 vol% oxygen indicates that the presence of water vapour leads to increasing conversion of CO at the expense of that of hydrogen. This behaviour may be due to the water gas shift reaction, where some CO reacts with water to form CO_2 and hydrogen.

3.7. *XRD of prepared catalysts*

XRD powder diffractograms were recorded for CuO, CuO/Al_2O_3, and the Pt/CuO/Al_2O_3 catalysts with different Pt content. In Fig. 7 the XRD patterns for pure CuO, CuO/Al_2O_3, and 4 wt% Pt/CuO/Al_2O_3 are shown. The CuO/Al_2O_3 shows reflections from CuO (JCPDS file no. 41-254) and γ-Al_2O_3 (JCPDS file no. 10-425) [21], and the 4 wt% Pt/CuO/Al_2O_3 sample and the Pt/CuO/Al_2O_3 samples with lower Pt content show the same reflections without any noticeable Pt peaks. The reflections from γ-Al_2O_3 are consistent with small crystallites. A surface area of 119 m^2/g corresponds to an average crystallite size of $\sim$ 14 nm. The absence of visible Pt peaks is mainly due a Pt content in the samples that is too small for detection by conventional powder XRD.

3.8. *TPR profiles*

A selection of recorded TPR profiles is displayed in Fig. 8. Reduction of the pure CuO gives a single peak with a maximum at 340 °C. Reduction of the CuO/Al_2O_3 sample gives a peak with a maximum at 230 °C, and a shoulder is noticeable on the high-temperature side of the peak at 255 °C. For the $Pt/CuO/Al_2O_3$ samples the maximum of the reduction peak shifts towards lower temperature with increasing Pt content, from 210 °C for 1.0 wt% $Pt/CuO/Al_2O_3$ to 160 °C for 4 wt% $Pt/CuO/Al_2O_3$. Similar to the reduction profile of CuO/Al_2O_3, those for the $Pt/CuO/Al_2O_3$ samples seem to be composed of at least two overlapping peaks. With increasing Pt content, the low-temperature portion of the reduction profile increases at the expense of the high-temperature part. Quantitative analysis of the hydrogen consumption corresponds to a CuO content of 20.4 wt% in the CuO/Al_2O_3 sample. As a result of Pt deposition, it seems that the CuO content is decreased somewhat. The reduction peaks for the $Pt/CuO/Al_2O_3$ samples correspond to CuO contents in the range of 15–17 wt% for these samples.

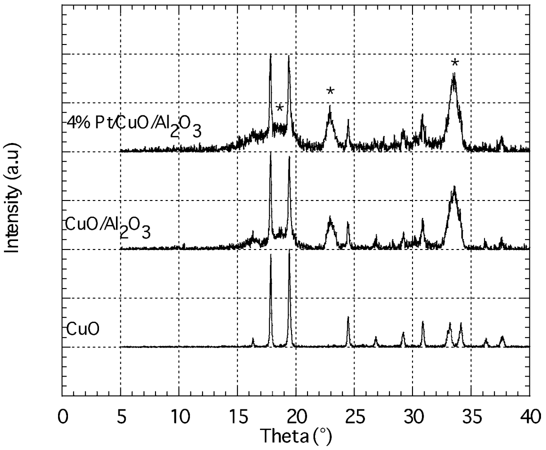

Fig. 7. XRD patterns of CuO, CuO/Al_2O_3 with 20 wt% CuO and 4 wt% $Pt/CuO/Al_2O_3$. The reflections from γ-Al_2O_3 are marked with (*) and all other peaks are from CuO.

3.9. *HREM and XEDS of catalysts*

At low magnification, the appearance of the catalysts is quite similar (Fig. 9), whereas the Pt particles become clearly visible at higher magnification (Fig. 10) because of the dark contrast and the typical lattice spacings of Pt. The size distribution of Pt particles is larger for the 4 wt% $Pt/CuO/Al_2O_3$ sample (roughly 2–50 nm) than for the 1 wt% $Pt/CuO/Al_2O_3$ sample (2–5 nm). The alumina support forms typical raft-like crystals with darker patches, which we interpret as areas richer in Cu, even though the Cu seems to be otherwise well dispersed over the surface. All elements in the samples were identified by XEDS. Elemental mapping was performed with Al K, Cu K, and Pt L radiation. To have clear visibility of the smallest Pt particles in STEM mode, instrumental magnifications between 1 and 2 million × had to be used, which limits the possibilities for X-ray maps with good counting statistics because of drift of the sample. Fig. 11 shows the result of HAADF imaging of the 1 wt% $Pt/CuO/Al_2O_3$ catalyst and mapping of Al, Cu, and Pt. There is a slight discrepancy in the maps of Al and Cu, supporting

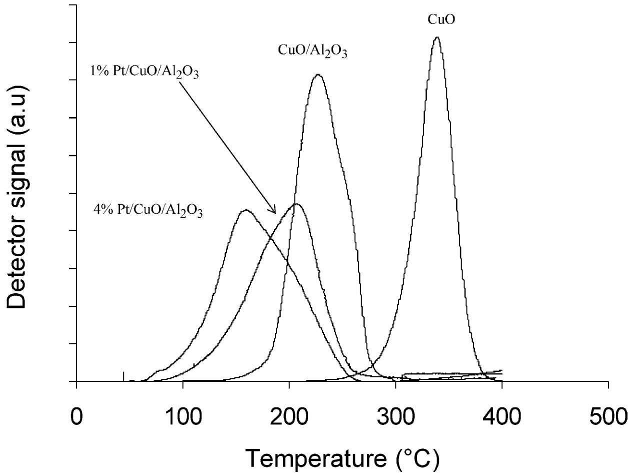

Fig. 8. TPR profiles for pure CuO, CuO/Al_2O_3 and $Pt/CuO/Al_2O_3$ with 1 and 4 wt% Pt.

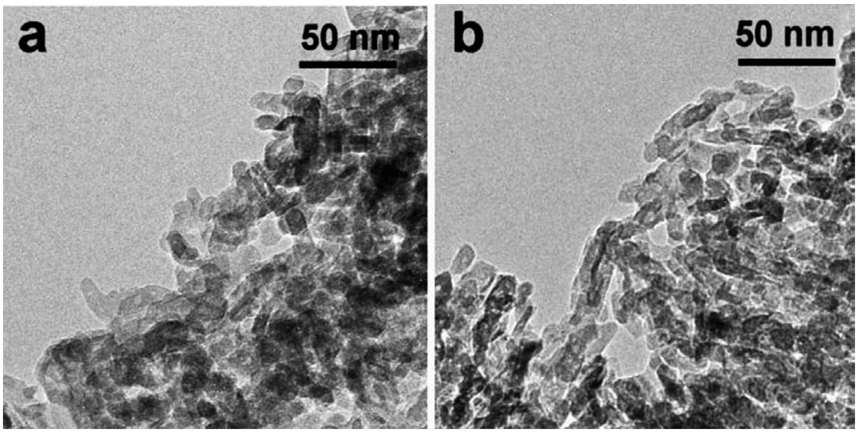

Fig. 9. TEM images of (a) CuO/Al_2O_3, and (b) 4 wt% $Pt/CuO/Al_2O_3$. The Cu content is 20 wt% in both samples. The images show no major differences in appearance at lower magnification.

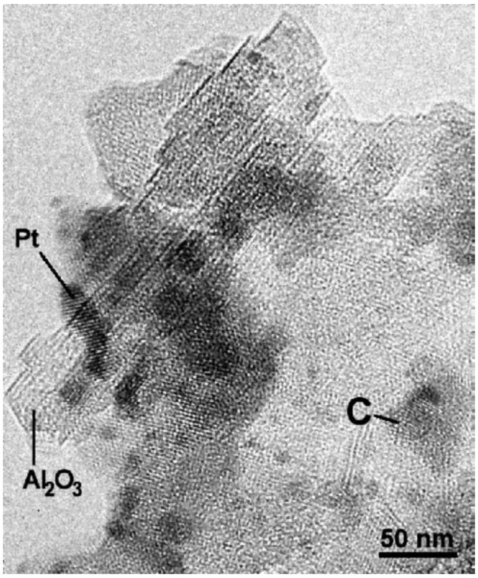

Fig. 10. HREM image of 4 wt% $Pt/CuO/Al_2O_3$. The darker Pt-particles are identified by the d_{111} fringes, which are measured as 0.218 nm in fair agreement with 0.226 nm in the literature. Crystallites of the alumina support are distinguishable. Darker patches (one marked C) presumably having a higher CuO_x content are frequent, and the Pt particles are primarily attached to these areas.

the idea of a patchwise occurrence of CuO_x. The 2–5-nm Pt particles can be distinguished in the Pt map, which has a tendency to follow the Cu map rather than the Al map.

To further verify the occurrence of Pt in conjunction with Cu, selective imaging of Pt was performed with large detection angles (116–309 mrad) for the HAADF imaging, followed by imaging at lower angles (57–152 mrad), where there is an increased Rutherford scattering contribution from Cu. Keeping above 50 mrad efficiently removes Bragg scattering from the image formation process. The result is shown in Fig. 12. The profiles show an increase in background from primarily the Cu content for the lower angle.

4. Discussion

4.1. Catalyst structure

HREM imaging of $Pt/CuO/Al_2O_3$ shows the patchwise occurrence of copper oxide on the alumina surface (Fig. 10). The presence of crystalline CuO in the catalysts is verified by the X-ray diffraction patterns in Fig. 7. Moreover, elemental mapping of Cu by HAADF imaging shows that

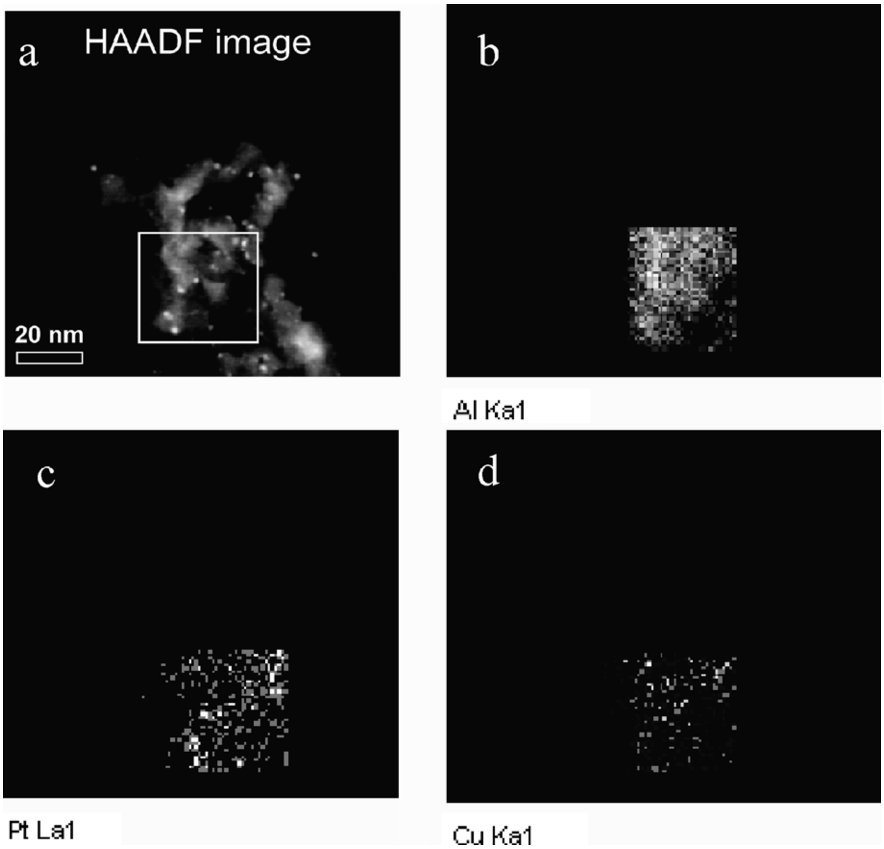

Fig. 11. Scanning transmission image and X-ray emission maps of 1 wt% $Pt/CuO/Al_2O_3$. (a) STEM image using a high-angle annular dark-field detector. The bright Pt particles are typically 2–5 nm in diameter. The boxed area was selected for mapping. (b) Mapping of Al detecting Al $K\alpha1$ radiation. (c) The map of Pt verifies the Pt particles in (a) and a distribution following the occurrence of the Cu shown in (d). Cu is well dispersed over the support material giving rather low counting statistics, being limited by the substantial drift of the specimen stage. Mo grids were used instead of the traditional Cu grids in order to reduce the stray Cu signal.

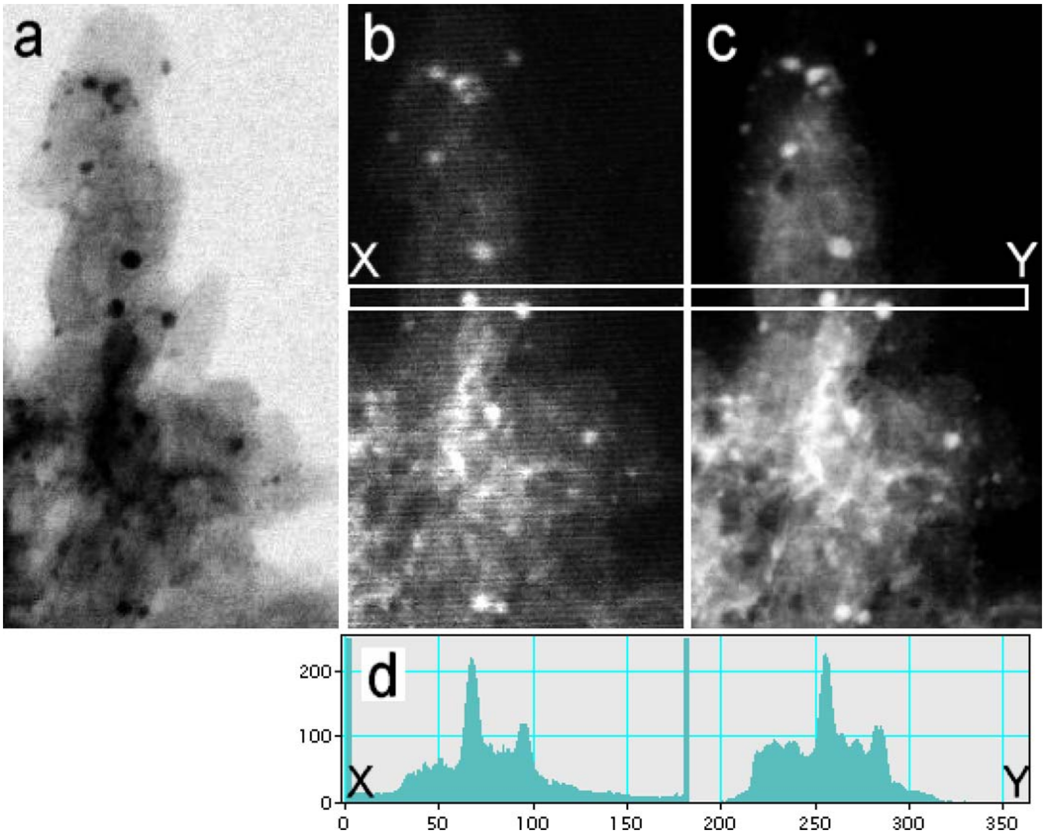

Fig. 12. STEM bright-field and dark-field images of 1 wt% Pt/CuO/Al_2O_3. (a) Bright field image including Bragg scattering. (b) HAADF image with a collection angle of 116–309 mrad, giving selective imaging of high-Z elements (e.g., Pt) through incoherent Rutherford scattering. (c) At lower collection angles (57–152 mrad) a larger contribution to image intensity is due to primarily the Cu content with a smaller contribution from Al. Bragg diffraction contrast is still excluded from the image. The intensity profile along the line trace X–Y is shown in (d). The profiles are normalised to the same particle, thus showing quantitatively the increased scattering contribution at this longer camera length from CuO_x and Al_2O_3 in areas surrounding the Pt particle.

copper is well dispersed on the alumina support and covers a large part of the surface (Fig. 11). The existence of well-dispersed copper oxide species is in agreement with the TPR profiles in Fig. 8, showing that the reduction peak for CuO on alumina is shifted towards lower temperature (230 °C) compared with that for bulk CuO (340 °C). Quantification of the reduction peak for CuO/Al_2O_3 verified that Cu is present as Cu(II). Thus, our results clearly demonstrate that copper on the alumina is present mainly in the form of CuO. No indications from XRD or HREM were obtained for the formation of a $CuAl_2O_4$ phase, which is in agreement with the report that formation of bulk $CuAl_2O_4$ requires heating above 700 °C [22]. However, on the basis of the Cu map in Fig. 11 we cannot exclude the possibility that a minor part of the Cu is present in the form of a surface copper aluminate phase. The formation of such a structure has been reported in the literature. Wolberg and Roth [22], using X-ray absorption spectroscopy, reported that for low surface concentrations of Cu on alumina, a surface phase is formed that resembles the structure of $CuAl_2O_4$. It was found that this phase is undetectable by XRD. Friedman and co-workers [23], in a comprehensive investigation combining various spectroscopic techniques, reported that in the copper aluminate surface structure the cupric ions are predominantly in a tetragonally distorted octahedral environment. In bulk $CuAl_2O_4$ 60% of the copper ions are in tetrahedral coordination and 40% are in octahedral coordination. The threshold value between the formation of the copper aluminate surface phase and the appearance of crystalline CuO is around 4 wt% Cu (∼ 5 wt% CuO) per 100 m^2/g of γ-Al_2O_3 [23,24]. Thus, considering that the CuO content in our catalysts is about 20 wt%, the appearance of strong XRD lines from CuO (Fig. 7) does not exclude the possibility that some of the Cu is in the form of a surface aluminate phase. The appearance of a main reduction peak at 230 °C with a shoulder at 255 °C in the TPR profile of CuO/Al_2O_3 (Fig. 8) gives some support for the existence of two types of copper species. Indeed, quantitative XRD measurements [25] have indicated that for copper concentrations above the threshold value, both the copper surface phase and CuO are present on alumina. In this regard it should be mentioned that in the literature there is some doubt about the formation of a copper aluminate surface phase. In an investigation of Ag/CuO/Al_2O_3 [15] the formation of such a phase was disregarded because of LEIS signal intensities.

The HREM and STEM results in Figs. 10–12 for Pt/CuO/Al_2O_3 show that the Pt is in the form of particles that are preferentially localised on areas with copper, which can explain the synergy between Pt and CuO on alumina that has been observed in the SCO of ammonia. In previous TPD experiments with adsorbed ammonia [26] we observed that the nitrogen formation peaks for CuO/Al_2O_3 and Pt/Al_2O_3 appear at higher temperatures than the 225 °C that is shown in Fig. 1 for $Pt/CuO/Al_2O_3$. Further support for the Pt particles being in direct contact with the copper species is given by the TPR profiles in Fig. 8 for 1 wt% $Pt/CuO/Al_2O_3$ and 4 wt% $Pt/CuO/Al_2O_3$. Compared with the reduction peak for CuO/Al_2O_3, the reduction peak for $Pt/CuO/Al_2O_3$ shifts towards lower temperature with increasing Pt content of the sample, suggesting spillover of hydrogen atoms from Pt to the copper species. The reduction peak for the $Pt/CuO/Al_2O_3$ samples is skewed, which can be explained by the reduction first of copper species in close contact with the Pt particles, followed by the reduction of more distant species. This explanation is in agreement with the observation that the low-temperature part of the reduction peak increases with increasing Pt content of the sample.

4.2. Catalytic performance of $Pt/CuO/Al_2O_3$

The TPD profiles in Fig. 1 for adsorbed ammonia and products indicate that $Pt/CuO/Al_2O_3$ is active and selective for nitrogen formation in the interval 200–250 °C. The data in Fig. 2 from flow experiments under stationary conditions confirm that almost complete conversion of ammonia is obtained at 200–230 °C, with a selectivity for nitrogen of about 85%. A comparison of the conversion curves in Fig. 2 for 1 wt% $Pt/CuO/Al_2O_3$ and 4 wt% $Pt/CuO/Al_2O_3$ reveals that the latter catalyst is only slightly more active than the former sample. This fact is in agreement with the observations in HREM that the size distribution of the Pt particles becomes wider with increasing Pt content on the support. When we consider the data in Fig. 2, we see that $Pt/CuO/Al_2O_3$ is more active for ammonia oxidation (700 ppm) at 0.5 vol% than at 8.0 vol% oxygen, indicating competitive adsorption of O_2 and NH_3. Since adsorbed O_2 is an electron-withdrawing species and NH_3 has a lone pair of electrons, competitive adsorption between the species implies that the adsorption site is a reduced species. In a previous mechanistic investigation [26] proofs were presented that the main route for the SCO of ammonia on $Pt/CuO/Al_2O_3$ involves reaction at the phase boundary between NH_x species adsorbed on Cu sites and oxygen adsorbed on Pt. Thus, poisoning of the ammonia adsorption site by oxygen suggests that this site is a reduced copper site (Cu^+). It has been verified by FTIR that ammonia is preferentially adsorbed as $NH_{3(ad)}$ on CuO/Al_2O_3 and that NH_4^+ species are much less abundant [1,16]. Under flow conditions with ammonia in the stream, bands from $NH_{3(ad)}$ were observed up to 350 °C [16] and up to 200 °C [1] under static conditions with adsorption followed by evacuation. These results are in line with the TPD profile of ammonia in Fig. 1, showing desorption of unreacted ammonia up to 250–300 °C.

For an oxygen content in the feed of 2.0 vol% and above, the plots in Fig. 3 show that at complete ammonia conversion the selectivity for nitrogen formation passes through a maximum when the temperature is increased. According to Fig. 4b the maximum is a result of the formation of N_2O passing through a minimum and the formation of NO_x simultaneously increasing with increasing temperature. The minimum in the N_2O formation agrees with the N_2O profile in Fig. 1, showing two peaks at 80 and 250 °C, respectively. Obviously, there are two different mechanisms for the formation of N_2O. The mechanism at low temperature may involve adsorbed O_2 species, whereas the formation at high temperatures is likely to involve monoatomic oxygen species. At low oxygen pressure the number of adsorbed O_2 species is scarce, explaining that the selectivity for nitrogen formation shows no maximum in Figs. 3a and 3b for low oxygen concentrations in the feed.

Considering the results in Fig. 5 and Tables 2 and 3 for high conversion conditions, it is evident that the addition of water vapour to the feed has almost no effect on the conversion of ammonia. Depending on the reaction conditions, the conversion either remains unchanged or shows a slight decrease with the addition of water vapour. On the other hand, the data also show that the selectivity for nitrogen in most cases is strongly improved by the addition of water. These findings are in general agreement with literature reports on several catalyst systems, for example, CuO/Al_2O_3 [10], Pt/Al_2O_3 [2], Pd-ZSM-5 [2], PdO/Al_2O_3 [2], $Pd–V_2O_5–WO_3/TiO_2–SiO_2$ [3], MoO_3/SiO_2 [7], and Fe-ZSM-5 [13]. The observed improvement of the selectivity for nitrogen in the presence of water can be seen as a consequence of the increase in the number of –OH groups at the surface relative to the number of oxygen species. For the successive stripping of hydrogen from adsorbed ammonia, only –OH groups are needed, whereas the formation of nitrogen oxides also requires oxygen species. This explanation agrees with our previous results [26], showing that the major route on $Pt/CuO/Al_2O_3$ for nitrogen formation proceeds via direct oxidation of ammonia involving two NH_x species without any participation of formed NO_x. In accordance with previous reports [7,10], the slightly reduced activity induced by water may be associated with competitive adsorption between ammonia and water. That the effect is minor can be explained by the stronger interaction of ammonia with the acidic adsorption sites when compared with the less basic water molecule. The present results are for high conversion conditions, and, therefore, the effect of water on the activity may be enhanced at lower conversion. However, the improved selectivity for nitrogen caused by water is not an effect of operating the catalyst below its capacity, because at low temperature nitrogen is an inert product that consequently does not react to form nitrogen oxides. Operation of a catalyst below full capacity is common practice in industrial applications, where it is a means of prolonging the lifetime of the catalyst load by increasing its tolerance towards poisoning.

Pretreatment of $Pt/CuO/Al_2O_3$ with SO_2 results in some reduction of the activity and considerable improvement of the selectivity for nitrogen, as the data in Table 2 show. Similar findings have been reported in previous investigations. A comparison of CuO/TiO_2 catalysts produced from $CuSO_4$ and $Cu(NO_3)_2$, respectively, showed that the catalysts had similar activity, but the former was more selective [8]. In a study of CuO/Al_2O_3 [10] it was found that introducing SO_2 into the feed gives improved selectivity and reduced activity. Moreover, data for $Pt/CuO/SiO_2$ demonstrate a strong boost of the selectivity for nitrogen when SO_2 is added to the feed [19]. For Fe_2O_3/TiO_2 similar trends were observed, and this whether the sample was prepared from sulphate or from nitrate and in the latter case subsequent treatment with SO_2- and O_2-containing gas [12]. These findings point to sulphate formation as the origin of the observed boost in the selectivity for nitrogen (Table 2). It is well known that CuO and Al_2O_3 interact with SO_2 to form sulphates [27,28]. Under our pretreatment conditions (see Section 2.2), assuming all SO_2 forms sulphate, the amount of sulphate corresponds to ~ 5 μmol/m^2 of surface area, that is, less than a monolayer. Therefore, most of the sulphate species in the catalysts can be expected to be in the form of surface species. These species seem relatively stable, as no worsening of the catalyst performance was observed during the time of the experiment (8 h). Sulphate surface species are electron withdrawing, resulting in an increase in the Lewis acid strength of the surrounding cation [12]. Thereby the surface concentration of adsorbed ammonia species is increased, facilitating the interaction between two adjacent nitrogen species forming N_2, in agreement with the experimental results in Table 2. The minor decrease in the activity that is observed after the pretreatment of the catalyst with SO_2 is in agreement with stronger interaction between nitrogen and the Cu ion, which would affect the desorption rate. The effect, however, is not strongly noticeable under the present reaction conditions with operation of the catalyst at high conversion. Moreover, replacement of some of the active oxygen sites with sulphate species may contribute to the observed changes in the catalyst performance. In particular, it would limit the minor secondary route to nitrogen formation on $Pt/CuO/Al_2O_3$, which comprises a reaction between an NH_x species and formed NO_2 [26].

Concerning the oxidation of ammonia in the presence of water and other biogas components (CO, H_2, and CH_4), the data in Table 3 show that almost complete conversion of ammonia is achieved, and the selectivity for nitrogen is 98 and 90% for feeds with 0.5 and 8.0 vol% oxygen, respectively. For the dry biogas with low oxygen content (0.5 vol%), compared with the corresponding wet gas, the conversion of ammonia is much lower (18%) and the selectivity for nitrogen is decreased from 98 to 87%. The decrease in the activity is a consequence of the oxygen content in the gas being almost completely consumed by the oxidation of CO and hydrogen to form CO_2 and water, respectively. Concerning the observed decrease in the selectivity for nitrogen, fewer –OH groups are expected to form at the surface when no water is fed. These species are active for the abstraction of hydrogen from ammonia and the formation of nitrogen, but they are not involved in the formation of CO_2, although they may affect to some extent the oxidation of hydrogen. As explained earlier, lowering of the OH/O surface ratio is in line with increasing the $(N_2O + NO_x)/N_2$ product ratio.

The data in Table 3 show complete conversion of the ammonia in a dry biogas feed with excess oxygen (8.0 vol%) and without added water. However, compared with the data for the corresponding feed with 0.5 vol% oxygen, a remarkable lower selectivity for nitrogen can be noticed (55% compared with 87%). The decrease seems to be related to the presence of CO, since a similar change with the oxygen content is obtained for the feeds with ammonia and CO only (see also Fig. 6). Also in that case the selectivity drops when the oxygen content is increased from 0.5 to 8.0 vol%, whereas no corresponding decrease is observed with a feed of ammonia and oxygen only. In the latter case complete conversion of ammonia is obtained at both oxygen levels, and in both cases the selectivity for nitrogen is about 90%. The low selectivity for nitrogen formation in the presence of CO and excess oxygen is surprising but is possibly related to formation of carbonate species [29–31] directing the reaction towards formation of nitrogen oxides, with N_2O as the main component. Carbonate species may also form without excess oxygen in the feed (0.5 vol%). In that case, however, the substantially higher selectivity for nitrogen may be due to the reaction of the formed nitrogen oxides with CO to give nitrogen and CO_2. Thus, under oxygen-rich conditions it seems that CO preferentially does not react with NO_2 but reacts with oxygen.

5. Conclusions

The present study has shown that $Pt/CuO/Al_2O_3$ is active and selective for the oxidation of ammonia to form nitrogen. At a space velocity on the order of 3600 ml/(min g), corresponding to 240 000 h^{-1}, full conversion of ammonia is obtained at 220–260 °C, with selectivities for nitrogen in the range of 85–90%. Adding water vapour to the feed gives improved selectivity for nitrogen (90–95%) and decreases the activity, although the effect on the conversion is small at high conversion levels. The fact that the catalyst is active below 300 °C and at high space velocity makes it very competitive with other catalyst systems [2,3,6–17]. Compared with Pt/Al_2O_3 [2], $Pt/CuO/Al_2O_3$ is more selective, and it is also much more active than CuO/Al_2O_3 [9,10], indicating a cooperative action between Pt and copper oxide. HREM imaging combined with elemental analysis of the catalyst shows intimate contact between platinum particles and copper-rich areas, facilitating cooperation between the phases.

Sulphating the catalyst by treatment with SO_2/O_2 makes it more selective for nitrogen formation and slightly less active. A selectivity of about 97–98% is obtained at complete ammonia conversion.

Concerning application of Pt/CuO/Al_2O_3 for the SCO of ammonia in biogas, our investigation shows that under wet conditions the catalyst efficiently converts the ammonia to nitrogen with good selectivity (90–98%, depending on the oxygen content). Under dry conditions, however, the catalyst has either low activity for ammonia oxidation or low selectivity for nitrogen formation, depending on whether the oxygen content in the feed is low or high.

Acknowledgments

The Swedish Research Council is acknowledged for financial support. LRW acknowledges support from the Knut and Alice Wallenberg Foundation.

References

[1] L.I. Darvell, K. Heiskanen, J.M. Jones, A.B. Ross, P. Simell, A. Williams, Catal. Today 81 (2003) 681.
[2] Y. Li, J.N. Armor, Appl. Catal. B 13 (1997) 131.
[3] M. Ueshima, K. Sano, M. Ikeda, K. Yoshino, J. Okamura, Res. Chem. Intermed. 24 (1998) 133.
[4] C.N. Satterfield, Heterogeneous Catalysis in Industrial Practice, second ed., McGraw-Hill, New York, 1991, pp. 312–320.
[5] J.M. Bradley, A. Hopkinson, D.A. King, J. Phys. Chem. 99 (1995) 17032.
[6] J.J.P. Biermann, F.J.J.G. Janssen, M. de Boer, A.J. van Dillen, J.W. Geus, E.T.C. Vogt, J. Mol. Catal. 60 (1990) 229.
[7] L. Lietti, G. Ramis, G. Busca, F. Bregani, P. Forzatti, Catal. Today 61 (2000) 187.
[8] N.N. Sazanova, A.V. Simakov, T.A. Nikoro, G.B. Barannik, V.F. Lyakhova, V.I. Zheivot, Z.R. Ismagilov, H. Veringa, React. Kinet. Catal. Lett. 57 (1996) 71.
[9] L. Gang, J. van Grondelle, B.G. Anderson, R.A. van Santen, J. Catal. 186 (1999) 100.
[10] T. Curtin, F. O'Regan, C. Deconinck, N. Knüttle, B.K. Hodnett, Catal. Today 55 (2000) 189.
[11] M. Amblard, R. Burch, B.W.L. Southward, Appl. Catal. B 22 (1999) L159.
[12] R.Q. Long, R.T. Yang, J. Catal. 207 (2002) 158.
[13] R.Q. Long, R.T. Yang, Chem. Commun. (2000) 1651.
[14] R.Q. Long, R.T. Yang, J. Catal. 201 (2001) 145.
[15] L. Gang, B.G. Anderson, J. van Grondelle, R.A. van Santen, W.J.H. van Gennip, J.W. Niemantsverdriet, P.J. Kooyman, A. Knoester, H.H. Brongersma, J. Catal. 206 (2002) 60.
[16] M. Yang, C. Wu, C. Zhang, H. He, Catal. Today 90 (2004) 263.
[17] S.D. Lin, A.C. Gluhoi, B.E. Nieuwenhuys, Catal. Today 90 (2004) 3.
[18] R. Burch, B.W.L. Southward, J. Catal. 195 (2000) 217.
[19] F. Dannevang, US Patent 5 587 134 (1996), to Haldor Topsøe A/S, Denmark.
[20] J.T. Gleaves, G.S. Yablonskii, P. Phanawadee, Y. Schuurman, Appl. Catal. A 160 (1997) 55.
[21] JCPDS International Centre for Diffraction Data, Powder Diffraction File, Swarthmore, PA, 1991.
[22] A. Wolberg, J.F. Roth, J. Catal. 15 (1969) 250.
[23] R.M. Friedman, J.J. Freeman, F.W. Lytle, J. Catal. 55 (1978) 10.
[24] B.R. Strohmeier, D.E. Leyden, R.S. Field, D.M. Hercules, J. Catal. 94 (1985) 514.
[25] P.W. Park, J.S. Ledford, Appl. Catal. B 15 (1998) 221.
[26] G. Olofsson, A. Hinz, A. Andersson, Chem. Eng. Sci. 59 (2004) 4113.
[27] G. Centi, A. Riva, N. Passarini, G. Brambilla, B.K. Hodnett, B. Delmon, M. Ruwet, Chem. Eng. Sci. 45 (1990) 2679.
[28] S.M. Jeong, S.H. Jung, K.S. Yoo, S.D. Kim, Ind. Eng. Chem. Res. 38 (1999) 2210.
[29] F. Acke, B. Westerberg, L. Eriksson, S. Johansson, M. Skoglundh, E. Fridell, G. Smedler, Stud. Surf. Sci. Catal. 116 (1998) 285.
[30] A. Manasilp, E. Gulari, Appl. Catal. B 37 (2002) 17.
[31] J.W. Park, J.H. Jeong, W.L. Yoon, Y.W. Rhee, J. Power Sources 132 (2004) 18.